Electron transfer in surfactant films on electrodes; copper phthalocyaninetetrasulfonate–didodecyldimethylammonium bromide

James F. Rusling *, David J. Howe

Department of Chemistry, Box U-60, University of Connecticut, Storrs, CT 06269-3060, USA

Received 7 April 1994

Abstract

Ordered surfactant films on electrodes are promising for various applications, including catalysis, sensors and fundamental studies. The first part of this paper provides a short review of recent results on electron transfer in surfactant and surfactant-like films on electrodes. The second part of the paper describes an electrochemical study of cast films of copper phthalocyaninetetrasulfonate (CuPCTS) and the water-insoluble surfactant didodecyldimethylammonium bromide (DDAB). Films were prepared by first casting the DDAB films onto electrodes, then introducing the CuPCTS by ion exchange from solution, or by casting the films as the CuPCTS(didodecyldimethylammonium)$_4$ salt. Electrochemical behavior depends upon the method of preparation, which influences the structure of the film. The salt films were characterized by overlapped voltammetric peaks, while the ion exchanged films showed a well-resolved first reduction process. Analysis of voltammetric data at pH 12 showed that charge transport diffusion and electron transfer kinetics were significantly faster in the ion exchanged films than in the salt films. The fluid lamellar liquid crystal structure of the ion exchanged films facilitates charge transport compared to the salt films which are not liquid crystalline.

Keywords: Electron transfer; Surfactant film; Electrode; Copper complexes; Phthalocyanine complexes

1. Introduction

The word surfactant is short for surface-active agent. Surfactants are molecules with non-polar regions and charged or polar head groups (Fig. 1). These amphiphilic molecules adsorb strongly at solid/solution interfaces such as electrodes [1]. They have been employed in electrochemistry for many years. For example, surfactants minimize anomalous current maxima in polarography. They suppress these convection currents by adsorbing to the mercury/solution interface.

Surfactants were reported to influence the course of electron transfer reactions as early as 1952, when Holleck and Exner [2] showed that surface active agents inhibit reduction of nitroanaline anion radical formed by reduction of nitroanaline at a mercury electrode. Baizer reported in 1964 that large concentrations of tetraethylammonium p-toluenesulfonate facilitated one-electron electrochemical dimerization of adiponitrile, which

undergoes a two-electron reduction at lower electrolyte concentrations [3]. Similar selectivity can be achieved by using very small amounts of surfactant [4]. Baizer's discovery provided an inexpensive route to acrylonitrile, a precursor in the manufacture of Nylon, and is organic electrochemistry's largest commercial success [5]. The processes described above are two of the first examples of controlling electron transfer processes by surfactants adsorbed onto electrodes.

Despite these early successes, widespread interest in the fundamentals of electron transfer involving surfactant films and ordered surfactant-like coatings on electrodes has been relatively recent [1,6–9]. Understanding has lagged behind applications. A review of research in this area up to 1978 [6] reveals that attempts to relate apparent heterogeneous rate constants for electron transfer to the fraction of surfactant coverage on the electrode were only partly successful.

Recent work on electron transfer in surfactant films on electrodes has begun to focus on molecular based interfacial models within the context of modern theories
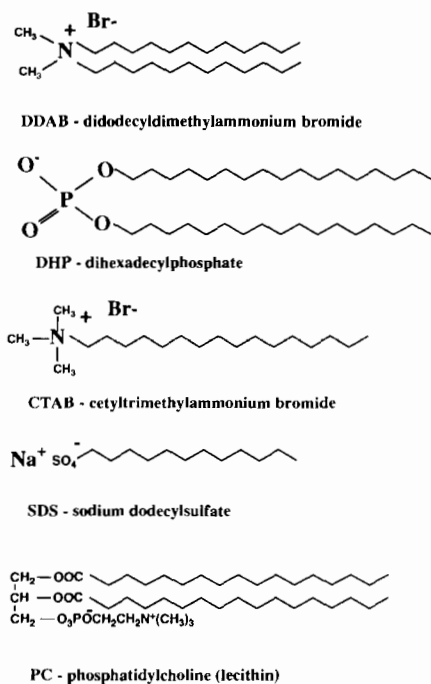
---

* Corresponding author.

DDAB - didodecyldimethylammonium bromide

DHP - dihexadecylphosphate

CTAB - cetyltrimethylammonium bromide

SDS - sodium dodecylsulfate

PC - phosphatidylcholine (lecithin)

Fig. 1. Structures of some typical surfactants.

admicelle   hemimicelle

Fig. 2. Proposed structures of surfactant films adsorbed onto charged surfaces. Circles are charged head groups, wiggly lines are hydrocarbon tails.

$$A_M \;\; + \; n\,e^- \;\rightleftharpoons\; B_M$$
$$+M \updownarrow \qquad\qquad\qquad +M \updownarrow$$
$$A_W \;\; + \; n\,e^- \;\rightleftharpoons\; B_W$$

Scheme 1.

of electron transfer [1]. Model systems involving ordered films prepared on electrodes are related to films which adsorb onto electrodes in surfactant solutions. In the first part of this paper, we briefly review recent studies pertaining to electron transfer in surfactant or related films on electrodes. In the second part, we discuss new studies on electron transfer involving a metal phthalocyanine in cast surfactant films on electrodes.

2. Recent studies of electron transfer in surfactant films

2.1. Adsorption of surfactants on electrodes

There are two experimental approaches to study electron transfer in surfactant films. First, experiments can be done on electrodes with surfactant coatings adsorbed from solutions. Second, ordered surfactant or surfactant-like films can be prepared on electrodes, and these systems can be studied in electrolyte solutions. In both cases, structural characterization of the coating on the electrode is important to facilitate a molecular interpretation of electrochemical data.

For ionic surfactants adsorbed onto charged surfaces from aqueous solutions at or above the critical micelle concentration (CMC), there is considerable electrochemical, spectroscopic and physical evidence for the arrangement of the surfactant molecules in bilayers [1,8]. These bilayers are called admicelles (Fig. 2), and feature a molecular layer with head groups down on the surface and a second layer with head groups facing
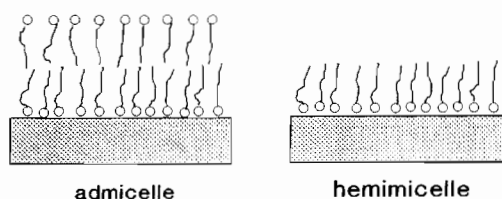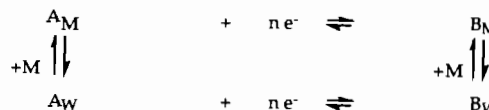
the solution. Hemimicelles feature a single surfactant layer with hydrocarbon chains facing the water. They have been proposed for adsorbates in solutions below the CMC when coulombic interactions between head groups and surfaces are very strong [10].

Practical electrochemical applications often involve relatively large surfactant concentrations. Under such conditions, especially at extreme potentials of opposite charge to that of the surfactant head group, evidence for multilayer films has been reported [1,10]. Such films can preconcentrate electrochemical reactants from solution by coulombic and hydrophobic interactions.

Films of surfactant-like molecules can be prepared on electrodes by chemisorption. For example, long chain thiols and disulfides form ordered monolayer films on gold electrodes via S–Au bonds [11]. Films can be prepared on oxidized electrode surfaces by reacting them with long chain trichlorosilanes [12]. Langmuir–Blodgett films can be transferred to electrodes [7,8]. Ordered films of water-insoluble surfactants can be cast onto electrodes [13]. These electrode coating methods have a broad range of interesting applications. In the context of this paper, they can be used for fundamental electron transfer studies when electroactive species are incorporated.

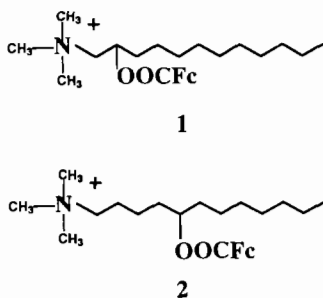### 2.2. Electron transfer in surfactant solutions

Electrochemical reduction or oxidation of reactants bound to surfactant aggregates such as micelles in solution are influenced by a variety of equilibria. Scheme 1 has been used to describe electrode reactions for a reactant A reduced to B in a solution containing micelles M [1,9]. Subscripts M and W refer to species bound to micelles or in water, respectively. In Scheme 1, both micelle-bound and free reactant may be reduced at the electrode. Equilibria of A and B with micelles must be taken into account in order to fully interpret electrochemical data. These equilibria are generally fast. Reactant dissociation from a micelle occurs on the ms

to μs time scale, and recapture of a reactant by a micelle is diffusion controlled [1].

On the other hand, results for several systems suggest that dissociation of reactants from micelles occurs prior to electron transfer [14–16]. Furthermore, it was necessary to consider more than one bound reactant per micelle to explain electrochemical diffusion coefficient data in micellar solutions [17]. As will be discussed below, electroactive reactants may also enter into surfactant coatings on electrodes prior to electron transfer [18]. Thus, the total picture concerning electron transfer in surfactant solutions is quite complex, and is not yet fully understood.

Several recent qualitative studies were aimed at investigating the influence of adsorbed surfactants on electron transfer rates. Voltammetry of inorganic [19] and organic [20] ions suggested somewhat enhanced electron transfer rates in the presence of surfactants with head groups of the opposite sign from the electroactive ions. Inhibition of electron transfer was observed if the sign on the ion and the surfactant was the same. Non-polar ferrocene and a partly hydrophobic organic ion showed a small amount of preconcentration on the electrode. Results are consistent with coulombic and hydrophobic interactions of the reactants with adsorbed layers of surfactant on the electrodes [19,20].

Abbott et al. [18] addressed fundamental questions concerning electron transfer in micellar solutions by studies on the C-12 ferrocenyl (OOCFc) surfactants 1 and 2 below.

1

2

Spectroscopic studies showed that 1 and 2 had similar interactions with CTAB micelles in solution. Heterogeneous electron transfer (ET) rate constants of ferrocene (Fc), 1 and 2 were nearly the same in homogeneous organic solvent at Pt electrodes, suggesting that no reactant orientation occurred on the electrode in these homogeneous solutions. However, in micellar CTAB solutions, electron transfer rate constants were found in the order Fc > 1 > 2, with approximately 10-fold differences between each compound. Activation free energies estimated from the dependence of the rate constants on temperature in CTAB micelles indicated similar reorganization energies for 1 and 2 during electron transfer (ET). Marcus theory predicts an exponential decrease of the rate of electron transfer as the distance between the electrode and the elec-

troactive species increases. Thus, these results suggest that the differences in rates are caused by differences in the distance of electron transfer in the sequence Fc < 1 < 2. A model featuring CTAB adsorbed onto the electrode with coadsorbed 1 and 2 oriented with head groups down on the electrode explains the data.

Electron transfer rates for 1 and 2 in CTAB solutions were consistent with the distance dependence predicted by Marcus theory using through space or through bond models [18], assuming that the molecules were oriented head group down on the electrode. Results imply that a small reactant like Fc enters a surfactant film on the electrode and approaches the electrode surface closer than does the Fc moiety of adsorbed 1. Since Fc, 1 and 2 are strongly bound to CTAB micelles in solution, some process by which the micelle-bound Fc reactant enters into a surfactant film on the electrode before electron transfer is inferred.

2.3. Electron transfer in chemisorbed and Langmuir–Blodgett (LB) films

In this section, we discuss several investigations which provide insight into mechanisms of electron transfer in adsorbed surfactant films. The advantage of working with chemisorbed, cast or LB films is that they can often be studied in electrolyte solutions free of surfactant and reactant. Thus, the micelle-reactant equilibria in Scheme 1 are eliminated, and the electrode process may be simplified.

Interesting studies have been done on metal electrodes coated with monolayer films via thiol or disulfide linkages. These films are conceptually similar to hemimicelles (Fig. 2). Li and Weaver attached a series of pentaammineCo(III) complexes to Au and Hg electrodes through thioalkylcarboxylate ligands [21]. While these compounds had chain lengths too short to be considered surfactants, results demonstrated an exponentially decreasing heterogeneous rate constant for electron transfer as the distance between the Co(III) center and the electrode increased, as predicted by Marcus theory.

Miller et al. coated gold electrodes with monolayers of hydroxy-terminated alkylthiols with chain lengths of 2 to 16 carbons [22]. They showed that heterogeneous electron transfer rates for oxidation of ferrocyanide and Fe^{2+} in solution decreased with increasing alkyl chain length.

Chidsey et al. prepared highly ordered mixed monolayer alkylthiol films, with some of the chains terminating in ferrocenyl groups [23]. These films were used to estimate the reorganization energy for electron transfer and the electron tunneling prefactor for the electroactive centers in the films [24a]. A recent report suggests that similar coatings on silicon electrodes show more efficient electron transfer when the hydrocarbon tails are in

highly ordered all-*trans* configurations compared to more disordered films [24b].

In situ studies of electroactive LB films were first done by Fujihara and Araki [25a], and shortly after by Majda and co-workers [25b]. LB films can also be coated onto electrodes [8]. In a study aimed at elucidating the influence of distance on electron transfer, Zhang and Bard transferred LB films made from Ru(bpy)$_2$(bpyC19)$^{2+}$ onto electrodes [25c]. Multilayers arranged in a head(down on electrode)–tail–tail–head–head–tail fashion showed faster electron transfer than repeated tail–head–tail–head orientations. However, the films with the electroactive head group down on the electrode showed electron transfer only to Ru(bpy)$_2$(bpyC19)$^{2+}$ in the first layer. In the case of repeated tail–head–tail–head orientations, at least three electroactive layers could be addressed electrochemically. These results are also in line with the exponential decay of rate constants with distance, since in the head(down on electrode)–tail–tail–head films, the second layer of head groups are too far from the electrode, or from the first layer of head groups, to exchange electrons with them [25c].

2.4. Electron transfer in cast surfactant films

Recent work in our laboratory explored the properties of self-assembled films of insoluble surfactants with the goal of applications to electrochemical catalysis. Films are prepared by casting solutions of the surfactants onto electrodes. These films are rather thick supramolecular aggregates resembling stacks of biological membranes. Their structures feature surfactant bilayers. With incorporated catalysts, these films can provide stable, fluid, catalytic coatings on carbon electrodes which have potential applications as sensors, in chemical conversions, and in developing new materials. In their liquid crystal states, these films exhibit excellent charge and mass transport [13,26].

Comparative electron transfer studies have been done with the protein myoglobin incorporated into cast films of didodecyldimethylammonium bromide (DDAB) on carbon electrodes. Myoglobin contains an Fe(III)heme group. Electron transfer rates for myoglobin in DDAB films increased up to 1000-fold over those obtained for myoglobin in solution on indium tin oxide electrodes [27]. Myoglobin has a secondary structure similar to its native, high-spin state and has a preferred orientation in the DDAB films [27,28]. Enhancement of electron transfer in the film may be related to the adsorption of the surfactant at the electrode/film interface and to orientation of the protein. Enhancement of electron transfer for myoglobin was also found in adsorbed films of water soluble surfactants such as SDS and CTAB [27], and in insoluble cast films of dihexadecylphosphate and lecithin.

Qualitative studies done on similar films of cationic surfactants with metal phthalocyanine tetrasulfonates incorporated by ion exchange suggest that stable films are formed with useful electron transfer properties [13,26,29]. The remainder of this paper describes a comparative study of electron transfer and charge transport in films prepared from copper phthalocyanine tetrasulfonate and DDAB by two different methods. Comparisons are also made to films of the phthalocyanine tetrasulfonate adsorbed onto bare electrodes in water.

3. Experimental

Phosphate buffers with ionic strength of 0.3 M were prepared from NaOH (Aldrich 99.99%) and H$_3$PO$_4$ (Baker Analyzed Reagent) using either a Corning model 130 or a Fisher Accumet model 910 pH meter with a Fisher model 13-620-104 combination electrode to measure pH. NaBr (Aldrich 99+%) was used to prepare 0.1 M NaBr(aq.) for Ag/AgBr reference electrodes. KCl (Fisher Certified ACS) was used to prepare saturated calomel reference electrodes (SCEs). Copper phthalocyanine-3,4′,4″,4‴-tetrasulfonic acid tetrasodium salt (CuPCTSNa$_4$) was from Aldrich. Didodecyldimethylammonium bromide (DDAB, 99%) was from Kodak, and chloroform was Baker Analyzed Photrex Reagent. All aqueous solutions were prepared from distilled/deionized water with a specific resistance ≥16MΩ cm.

The CuPCTS(DDA)$_4$ salt was prepared by exchanging the sodium ions in CuPCTSNa$_4$ for DDA$^+$ ions in a two phase water/chloroform extraction, using known masses of CuPCTSNa$_4$ in water and DDAB in chloroform. CuPCTS(DDA)$_4$ was recovered in the chloroform phase, and washed repeatedly with portions of water until no precipitate was obtained upon addition of AgNO$_3$ to the water layer, suggesting that all the Br$^-$ had been removed from the organic layer. The water extracts contained almost no color, indicating that only water insoluble CuPCTS(DDA)$_4$ remained in the organic phase, which also contained almost all of the starting mass of CuPCTS. The chloroform phase was then evaporated to yield the solid salt.

Pyrolytic graphite (PG) disks of approximately 5 mm diameter (HPG, Union Carbide) were press fitted into the larger end of polypropylene micropipette tips (Perfector Scientific, CA, Cat. No. 1612) and sealed into place by carefully heating the PG with the tip of a hot soldering iron. The PG disks were then ground flat using 600 grit SiC paper (Mark V Laboratory) mounted onto a metallographic polishing wheel (Buehler, Cat. No. R1138A) rotating at the high speed setting. Electrodes were then polished to a high gloss using an

aqueous dispersion (2 g/500 ml) of 0.3 μm α-alumina (Buehler) applied to a green billiard cloth (Mark V Laboratory) rotating at high speed on the polishing wheel. Finally, the PG electrodes were rinsed with distilled water and dried with a Kimwipe. Electrodes were coated with surfactant films by placing a droplet of 5 μl of the appropriate solution in chloroform onto inverted PG electrodes, slowly evaporating the solvent to visual dryness within a small glass chamber, then allowing them to stand in air overnight. Solutions were 9.9% by weight DDAB and 2% by weight CuPCTS(DDA)$_4$. Film thicknesses were estimated at 9 μm for DDAB and 7 μm for CuPCTS(DDA)$_4$ from the mass of material deposited and densities of 1.1 for CuPCTS(DDA)$_4$ and 1.0 for DDAB.

Adsorbed films were prepared by dipping PG electrodes held at 0.5 V in 10^{-5} M CuPCTS in buffer for 2 min at pH 2 and 3 min at pH 5 and 12, then washing with buffer.

Electrochemical measurements were done with a BAS 100 (Bioanalytical Systems) potentiostat or a PAR model 273 potentiostat/galvanostat (Princeton Applied Research) using maximum attainable compensation of the ohmic drop. Potentials of the Ag/AgBr reference electrodes relative to that of an SCE were measured with a Simpson model 461-2 digital multimeter using the electrochemical cell

Ag|AgBr(s)|0.1 M NaBr(aq.)|Agar|Buffer Solution| Agar|Buffer Solution|Agar|KCl(aq.), sat'd|Hg$_2$Cl$_2$(s), KCl(s)|Hg

containing the buffer solution to be employed in the subsequent electrochemical experiment. At pH 12, the Ag|AgBr(s), 0.1 M NaBr(aq.) reference electrode was -95 mV versus SCE. Salt bridge separators in electrochemical cells were agar gels supported by glass frits. Electrochemical cells were thermostated at 25 °C using a P.M. Tamson (Holland) circulating water bath and were blanketed under a positive pressure of N$_2$ from which oxygen had been removed. Working (coated PG) and counter (Pt wire) electrodes were used in a single cell compartment containing approximately 10 ml of electrolyte. The Ag/AgBr reference electrode was connected to the cell by a salt bridge containing the buffer solution of interest. Uncompensated ohmic drop was a maximum of <7 mV for the films at the highest scan rates, and less at lower scan rates. Differences in electrochemical parameters for the different types of films are unlikely to be influenced significantly by this source of error.

UV–Vis spectroscopy was carried out with a Perkin-Elmer Lambda 6 spectrometer. Spectra were taken in transmission mode for films cast onto quartz. Differential scanning calorimetry was done as described previously [29].

4. Results

4.1. Dependence of voltammetry on pH

Electrochemical reduction of copper phthalocyaninetetrasulfonate (CuPCTS) takes place by addition of electrons to the phthalocyanine ring [30]. Two separate one-electron reduction peaks in DMF were reported. The central copper(II) in CuPCTS is four-coordinate, and is thought not to accept axial ligands. Ring nitrogens are protonated only in very concentrated acid solutions [31]. The sulfonate groups are nearly completely ionized in the aqueous solutions of pH $\geqslant 2$ used in this work.

Films containing CuPCTS were prepared on polished pyrolytic graphite electrodes in three ways: (i) adsorption from an aqueous buffer solution (adsorbed CuPCTS); (ii) loading of CuPCTS by ion exchange from solution into a film of didodecyldimethylammonium bromide (DDAB) coated previously onto the electrode (ion exchanged CuPCTS–DDAB films); (iii) casting of a chloroform solution of CuPCTS(DDA)$_4$ onto the electrode, followed by evaporation of the solvent (CuPCTS(DDA)$_4$ salt films). Initial studies involved voltammetric and spectroscopic investigations over the pH range 2–12 in order to survey the properties of the films, and to identify conditions under which more detailed studies of electrochemical properties could be done.

Cyclic staircase voltammetry (CSV) imposes an overall triangular potential waveform onto the working electrode, with potential increments in tiny steps, and measures the resulting cell current near the end of each step. Under the conditions used in our work, CSV is nearly equivalent [32] to cyclic voltammetry (CV), and we shall refer to these experiments as CV. Square wave voltammetry (SWV) superimposes a repetitive sequence of a forward potential pulse followed by a reverse potential pulse upon a staircase potential input [33]. Current is measured at the end of each forward and reverse pulse. The voltammogram can be output as the difference current for each pulse sequence versus potential, or as forward and reverse current versus potential. The latter output resembles cyclic voltammetry. SWV was included because it provides better resolution and sensitivity than CV.

Films of adsorbed CuPCTS were studied after transfer of the coated electrode to buffer solutions not containing CuPCTS. Large negative shifts in reduction peak positions and changes in peak shape were found as pH was increased from 2 to 12 (Fig. 3). At pH 2, two severely overlapped SWV peaks are found at about -0.25 V versus SCE. At pH 5, three overlapped peaks were found in the -0.3 to -0.8 V region. At pH 12, a major peak is found at about -1 V.

These adsorbed films were unstable, and their signals gradually disappeared during voltammetric studies in
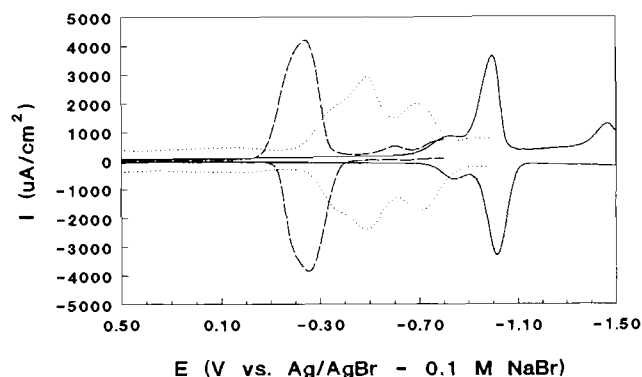
Fig. 3. SWV forward and reverse current–potential curves for adsorbed CuPCTS films on PG electrodes at pH values 12 (——), 5 (·····) and 2 (– – –) (frequency 150 Hz, pulse height 50 mV, step 2 mV).
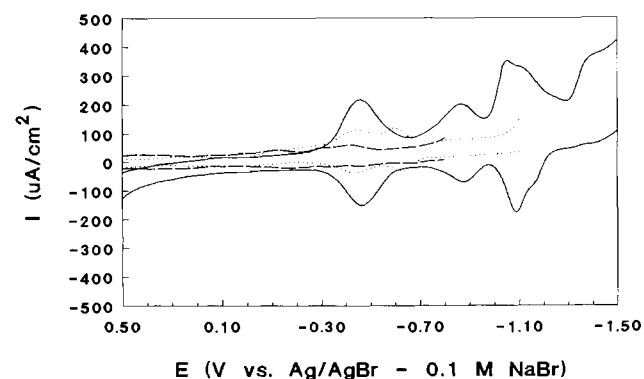

Fig. 4. SWV forward and reverse current–potential curves for ion exchanged CuPCTS–DDAB films on PG electrodes at pH values 12 (——), 5 (·····) and 2 (– – –) (frequency 150 Hz, pulse height 50 mV, step 2 mV).

Fig. 5. SWV forward and reverse current–potential curves for CuPCTS(DDA)₄ films on PG electrodes at pH values 12 (——), 5 (·····) and 2 (– – –) (frequency 150 Hz, pulse height 50 mV, step 2 mV).

with the addition of one electron to the phthalocyanine ring [29,30]. Thus, pH 12 was chosen for estimating electrochemical parameters of the films, as described below.

4.2. Thermal and spectroscopic characterization

Surfactant films and other surfactant aggregates arranged in bilayers exhibit a characteristic phase transition from a solid-like gel phase to the liquid crystal phase. In the gel state, the hydrocarbon tails of the surfactants are arranged in an all-*trans* conformation. Increasing temperature causes a cooperative transition to the fluid liquid crystal phase, featuring a significant population of bonds with gauche conformations in the hydrocarbon tails [34]. The phase transition temperature, T_c, is characteristic of the bilayers of specific surfactants and can be measured by differential scanning calorimetry (DSC).

The value of T_c for pure DDAB films was 11 °C, similar to the value of 15 °C for bilayer vesicles of DDAB [29]. Similarly, a T_c value of about 16 °C was measured by DSC for ion exchanged CuPCTS–DDAB films. These data suggest that DDA⁺ ions in the films are arranged in bilayers similar to the admicelles discussed earlier. Previously, scanning electron microscopy of cross sections of the films suggested that the bilayers may be arranged in stacks on the electrode surface [29]. In contrast, DSC studies of cast films of the salt CuPCTS(DDA)₄, either dry or after soaking in aqueous solutions, did not reveal phase transitions between 0 and 70 °C.

Phthalocyaninetetrasulfonates have a strong tendency to form face-to-face association dimers in aqueous solutions [35]. The presence of dimers is easily detected by visible absorbance spectroscopy. CuPCTS has a strong monomer absorbance band in water at 673 nm, and a main dimer band at about 625 nm [36]. Spectra of 0.01 mM CuPCTS in buffer solutions showed strong ab-

aqueous solutions. Film stability was pH dependent. Films at pH 2 were destroyed within 2 min. At pH 12, the films lasted for about 5 min, but successive scans revealed time dependent changes in the voltammograms.

Ion exchanged films of CuPCTS–DDAB showed smaller potential shifts with pH than the simple adsorbed films (Fig. 4) The first peak in the voltammograms remained close to −0.5 V from pH 5 to 12, but the secondary peaks changed significantly. The films were stable above pH 2 and gave reproducible voltammograms.

Cast films of CuPCTS(DDA)₄ and ion exchanged CuPCTS–DDAB films showed a similar pH dependence of the first major reduction peak. However, a somewhat different evolution of the shape and size of the secondary peaks with increasing pH was found for the CuPCTS(DDA)₄ films (Fig. 5).

The films of CuPCTS–DDAB and CuPCTS(DDA)₄ have superior stability to adsorbed films, and should be much more useful for practical applications. Both ion exchanged and salt films gave a relatively well separated first peak at pH 12 which can be associated
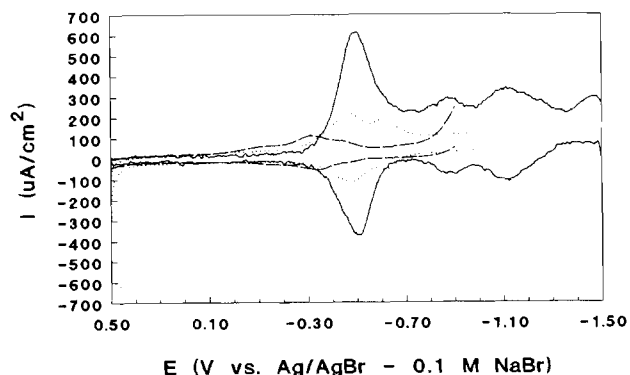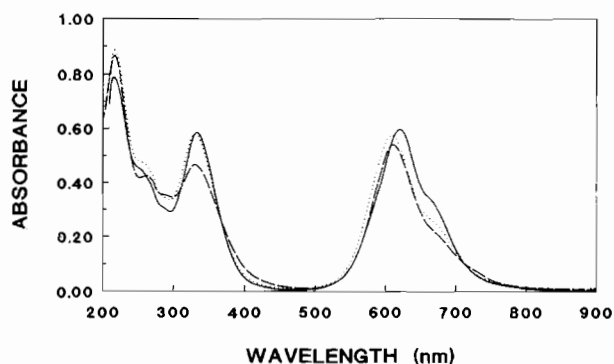
Fig. 6. Influence of pH on UV–Vis spectra of 0.01 mM CuPCTSNa$_4$ in solution: pH 12 (—), 5.3 (·····) and 2.1 (---).
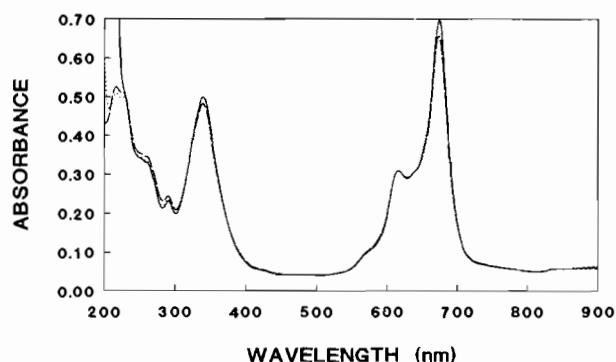

Fig. 7. Influence of pH on spectra of CuPCTS(DDA)$_4$ salt films: pH 12 (—), 5.3 (·····) and 2 (---).

sorbance bands close to 620 nm assigned to dimeric or oligomeric forms, and a shoulder near 670 nm which represents the monomer (Fig. 6). Ratios of the monomer to dimer absorbances suggest that CuPCTS is mainly in the form of aggregates in these solutions. A weak pH dependence of the spectra is observed, with the largest monomer to dimer peak ratio at pH 12. A small red shift was observed in the wavelength maximum of the dimer band with increasing pH. Small increases in absorbance with increasing pH were also found.

Visible spectra of CuPCTS–DDAB and Cu-PCTS(DDA)$_4$ films were similar to each other, but somewhat different from solution spectra at 0.01 mM. Overlapped bands were observed at about 610 nm which are attributed to dimer in the film (Fig. 7) [29]. The dimer band grows in as the loading of CuPCTS in the films is increased. However, the major band in the film spectra appears at about 670 nm and is assigned to the monomer. The monomer to dimer absorbance ratios suggest that the films soaked in buffer solutions contain much less dimer than 0.01 mM aqueous solutions. pH has little influence on the film spectra.

4.3. Electron transfer and diffusion studies

CV and SWV were done over a wide time scale range to compare the first reduction process in

CuPCTS–DDAB and CuPCTS(DDA)$_4$ films at pH 12. Quantitative analysis of such thick films on electrodes would be facilitated by observing a single electron transfer process under diffusion or diffusion-kinetic control, uncomplicated by associated chemical or electrochemical reactions. In such cases, it should be possible to obtain apparent heterogeneous electron transfer rate constants ($k°'$) from the separation of the anodic and cathodic peaks, and the charge transfer diffusion coefficients (D_{ct}) from the measured relation between peak current and scan rate [37]. Alternatively, a diffusion-kinetic model can be fit to individual voltammograms by non-linear regression [38] to obtain $k°'$.

Detailed voltammetric studies of the CuPCTS(DDA)$_4$ salt films showed that the single-electron transfer process observed in the medium frequency range (cf. Fig. 4) was accompanied by secondary processes. SWV for CuPCTS(DDA)$_4$ salt films at low frequency (analogous to low scan rates in CV) revealed a single set of forward and reverse peaks at about −0.50 V, with additional peaks at more negative potentials (Fig. 8(a)). However, upon increasing the frequency, a new peak at about −0.60 V grows in to severely overlap the first peak (Fig. 8(b)).

CV at scan rates less than 10 mV s^{-1} revealed two pairs of cathodic and anodic peaks in the region between −0.45 and −0.65 V versus SCE (Fig. 8(c)). When the scan rate was raised into the 0.1 to 2 V s^{-1} region (Fig. 8(d)), these peaks merge into an apparent single pair of cathodic–anodic peaks.

The voltammetric behavior of the ion exchanged CuPCTS–DDAB films was considerably different from the CuPCTS(DDA)$_4$ salt films. A single anodic–cathodic peak pair was found in the −0.3 to −0.45 V region throughout a wide range of SWV frequencies (Fig. 9(a) and (b)). At 10 Hz, a single pair of forward and reverse peaks near −0.4 V was found, and these peaks remained well resolved up to 500 Hz. Cyclic voltammetry between 1 mV s^{-1} and 5 V s^{-1} gave peaks with the familiar shape of a diffusion controlled process (Fig. 9(c) and (d)). No additional peaks were observed in high or low scan rate ranges as in the CuPCTS(DDA)$_4$ films.

Data from scan rate ranges where the most positive redox processes gave a well-resolved pair of cathodic–anodic peaks were analyzed to obtain estimates of $k°'$, D_{ct} and the electrochemical transfer coefficient (α). Plots of cathodic peak current versus square root of scan rate were reasonably linear (Fig. 10), and their slopes were used to estimate D_{ct} [37]. Also, cathodic–anodic separations of peaks with characteristic diffusion controlled shapes increased with increasing scan rate (Fig. 11). These results are consistent with the diffusion-kinetic model [39] at least in the range of scan rates where one pair of cathodic–anodic peaks is predominant.
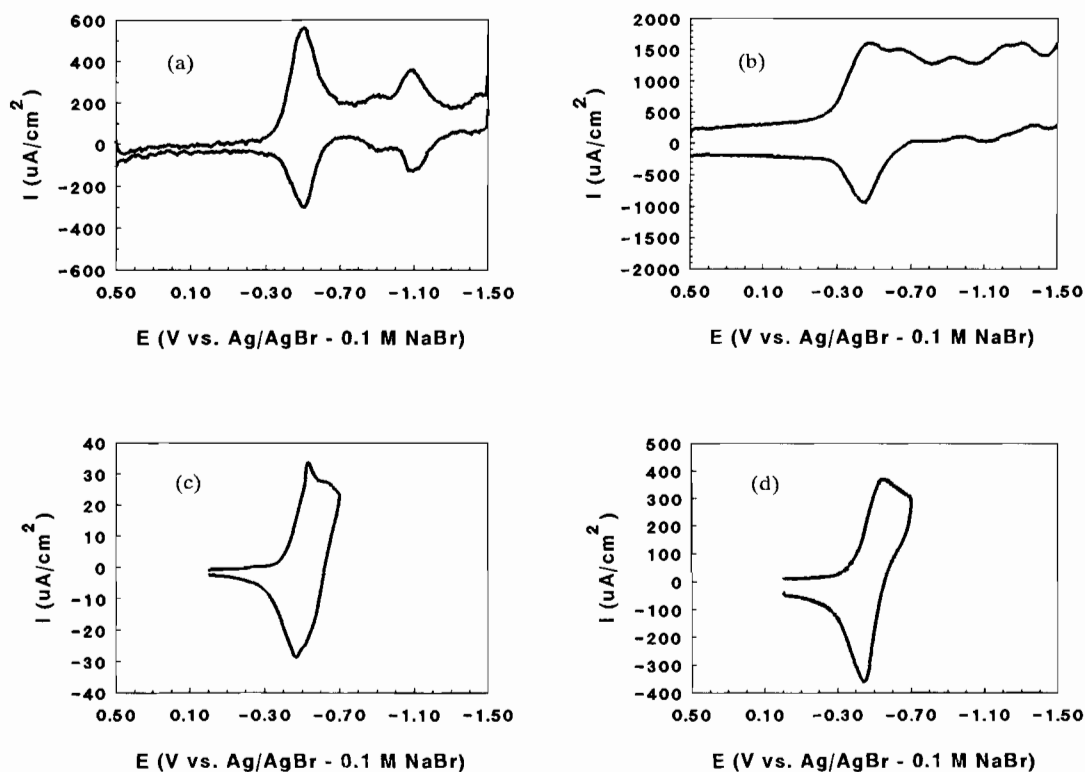
Fig. 8. Voltammograms of CuPCTS(DDA)$_4$ salt films in pH 12 phosphate buffer: (a) SWV at 10 Hz, pulse height 50 mV, step 10 mV; (b) SWV at 150 Hz, pulse height 50 mV, step 10 mV; (c) CV at 2 mV s^{-1}; (d) CV at 100 mV s^{-1}.
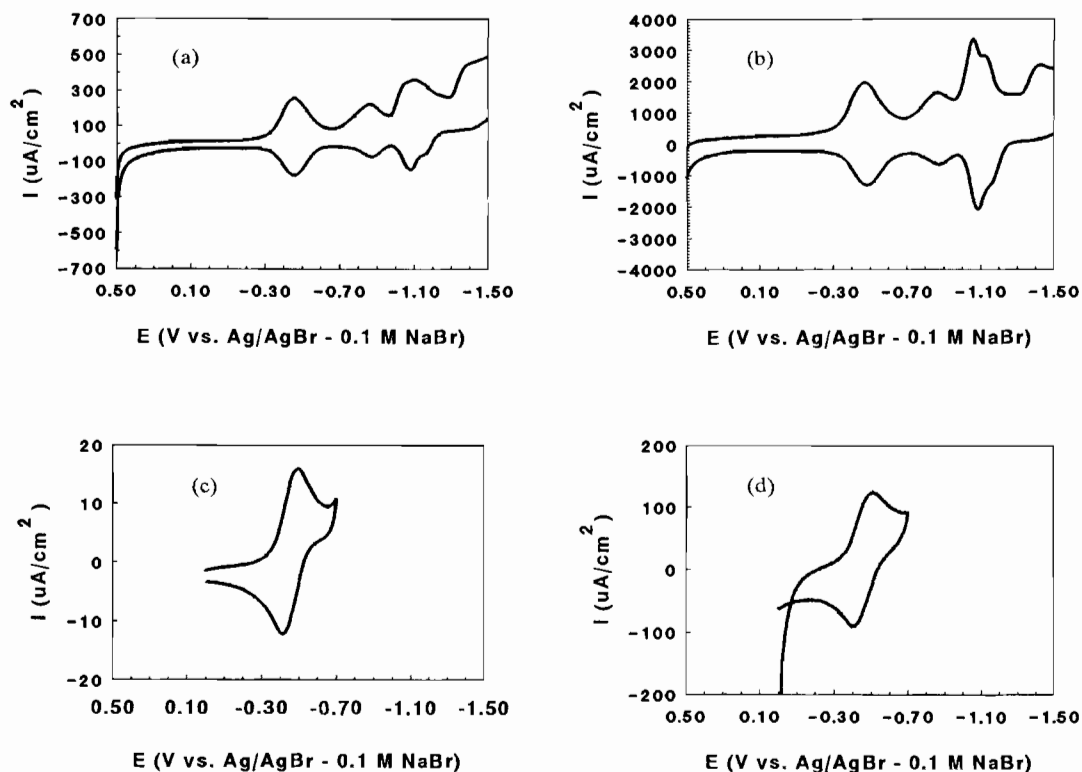
Fig. 9. Voltammograms of ion exchanged CuPCTS–DDAB films in pH 12 phosphate buffer: (a) SWV at 10 Hz, pulse height 50 mV, step 10 mV; (b) SWV at 150 Hz, pulse height 50 mV, step 10 mV; (c) CV at 2 mV s^{-1}; (d) CV at 100 mV s^{-1}.
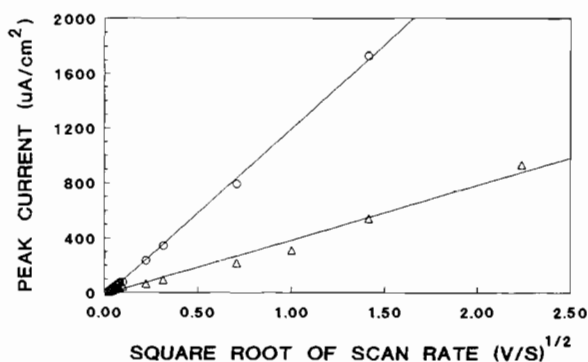
Fig. 10. Plot of CV peak current vs. square root of scan rate for ion exchanged CuPCTS–DDAB (△) and CuPCTS(DDA)$_4$ salt (○) films in pH 12 buffer.
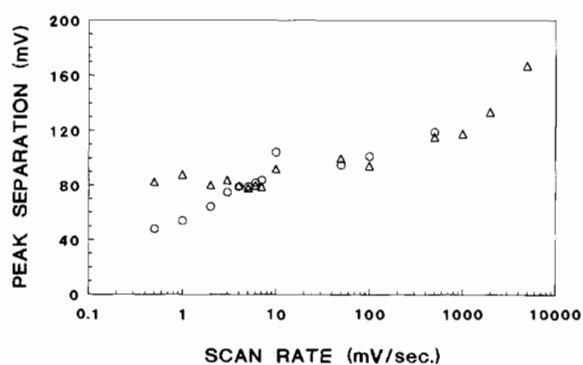

Fig. 11. Influence of scan rate on CV anodic–cathodic peak potential separation for ion exchanged CuPCTS–DDAB (△) and Cu-PCTS(DDA)$_4$ salt (○) films in pH 12 buffer.

Table 1

Electrochemical parameters estimated for CuPCTS–DDAB films at pH 12[a]

Parameter	Ion exchanged films	Salt films
ν range (V s^{-1})	0.0001–5.0	0.05–2.0
[CuPCTS], total (M)		0.47 ± 0.08
[CuPCTS][b], active (M)	0.02	0.28
D_{ct}[c] (cm^2 s^{-1})	5×10^{-9}	0.3×10^{-9}
$k^{o\prime}$ (cm s^{-1})	$3 \pm 2 \times 10^{-4}$	$0.4 \pm 0.2 \times 10^{-4}$
α	0.29 ± 0.04	0.25 ± 0.03

[a]Kinetic parameters obtained by fitting individual CVs by using the COOL algorithm and a kinetic-diffusion model (see Ref. [33]).
[b]CuPCTS estimated by coulometry at constant potential, divided by film volume estimated from amount deposited (see Ref. [13]).
[c]Charge transport diffusion coefficient assuming the same diffusion rate for oxidized and reduced forms of the films.

on coulometric estimates of CuPCTS concentration in the films (see Table 1) which contain considerable uncertainty. Thus, the kinetic parameters reported should be used only for comparison, and are not meant to represent absolute values.

Comparisons of the average kinetic parameters (Table 1) suggest that the two types of films have different electrochemical properties. Both the charge transport diffusion coefficient (D_{ct}) and the apparent electron transfer rate constant ($k^{o\prime}$) are about an order of magnitude larger for the ion exchanged film compared to the salt film.

5. Discussion

Results suggest that electron transfer and diffusion properties of surfactant films containing CuPCTS depend on the structure of the film. The structure of the film depends on the way in which the film is prepared. When DDAB films are prepared on the electrode first, and CuPCTS introduced by ion exchange from solution, the films are lamellar liquid crystals at room temperature. On the other hand, films cast from the Cu-PCTS(DDA)$_4$ salt are not liquid crystals and show complicated electron transfer behavior, with overlapped peaks in the vicinity of the first reduction process in both slow and fast voltammetric experiments. In intermediate time scale experiments, a single electrode process seems to predominate. The reasons for the overlapped peaks and for the observed pH dependence are not fully understood at present.

Electron transfer kinetics and charge transport appear to be faster for the ion exchanged films than for the salt films. The amount of electroactive CuPCTS in the ion exchanged films loaded in the pH 12 phosphate buffers is about 10-fold smaller than in the Cu-PCTS(DDA)$_4$ films, which have approximately a 1:4

Given the above results, we felt justified in using the diffusion-kinetic (or quasireversible) model to estimate kinetic parameters for the films. CV data were analyzed by using the COOL algorithm (PARC 271 software package), which provides best fits to individual CV scans and returns the values of kinetic parameters. The quality of the fits depends on using the correct model for the faradaic current as well as the ability to remove background signals from the data. Background correction was ignored in the present case, since a separate reproducible background representative of the films was difficult to obtain. In principle, background could be obtained with electrodes coated with surfactant alone. However, the presence of CuPCTS changes the film properties [29] and this approach was not considered applicable.

While reasonable matches between experimental and computed CVs were achieved upon convergence of the COOL algorithm, significant deviations from the model were found in many cases. We suspect that these deviations are partly caused by lack of background corrections and possibly by interfering faradaic processes not accounted for by the model. Thus, we have reported average results from these analyses to one significant figure only, and included standard deviations wherever possible (Table 1). Values of $k^{o\prime}$ and D_{ct} also depend

ratio of the CuPCTS to DDAB. Only a fraction of the CuPCTS in the salt film is electroactive (Table 1). Electronic spectra suggest that much less dimerization of the phthalocyanine occurs in the films compared to aqueous solution, but the degree of dimerization is similar in the two types of films. Decreased dimerization was also found for MPCTSs exchanged into DDAB films from neutral solutions [29], but some dimerization was necessary for retention of MPCTSs in the film.

Charge transport, as reflected by D_{ct} (Table 1), is significantly slower in CuPCTS–DDAB films than in liquid crystal films of DDAB containing ferrocyanide, a cyanocobalt corrinhexacarboxylate, or myoglobin [26]. This may be related to a structural role for metal phthalocyanines in MPCTS–DDAB films. We found previously that DDAB films containing MPCTSs were considerably more stable (e.g. several weeks) than DDAB films containing ferrocyanide or cyanocobalt corrinhexacarboxylate. The latter films retained their solutes for only a few hours after transfer to blank electrolyte solutions. If MPCTSs are more tightly bound in the film than are the other anions, they may have more difficulty in physically diffusing. Such a film may rely partly on an electron hopping mechanism to transport electrons rather than physical diffusion. Experiments are currently underway to answer this question.

The study presented here illustrates that the dependence of electron transfer kinetics and charge transport on surfactant film structure. The liquid crystal state of the film facilitates faster diffusion of charge, as would be expected from the increased fluidity of the lamellar liquid crystal state. The reason for slower electron transfer kinetics of the salt films is unclear, but may also be related to the structure of the films.

6. Conclusions

As discussed previously, electron transfer kinetics in films depends on the distance of the reactant from the electrode [18,21,22]. Electron transfer rates in LB films depended on the distance between electroactive centers within the film [25]. Diffusion of charge in DDAB films was found to be considerably faster in the liquid crystal state, as compared to the solid-like gel state [13,29].

The present work provides evidence that charge transport and electron transfer rates in cast surfactant films containing electroactive ions are improved in the fluid liquid crystal state, compared to phases which are not liquid crystalline. The increased molecular mobility within films in this phase apparently allows faster charge transport. The effect seems analogous to improved charge transport upon chain melting of electroactive polymers, which increases chain mobility [40].

References

[1] J.F. Rusling, in A.J. Bard (ed.), *Electroanalytical Chemistry*, Vol. 18, Marcel Dekker, New York, 1994, pp. 1–88.
[2] L. Holleck and H.J. Exner, *Z. Elektrochim.*, 56 (1952) 46.
[3] M.M. Baizer, *J. Electrochem. Soc.*, 111 (1964) 215.
[4] M.R. Moncelli, F. Pergola, G. Aloisi and R. Guidelli, *J. Electroanal. Chem.*, 143 (1983) 233.
[5] D.E. Danly, in M.M. Baizer and H. Lund (eds.), *Organic Electrochemistry*, Marcel Dekker, New York, 2nd edn., 1983, pp. 959–994.
[6] N. Shinozuka and S. Hayano, in K.L. Mitall (ed.), *Solution Chemistry of Surfactants*, Vol. 2, Plenum, New York, 1979, pp. 599–623.
[7] M. Fujihara, in A.J. Fry and W.E. Britton (eds.), *Topics in Organic Electrochemistry*, Plenum, New York, 1986, pp. 255–294.
[8] J.S. Facci, in *Techniques in Chemistry*, Vol. 22, (W.H. Saunders, (Series ed.), R.W. Murray (ed.), *Molecular Design of Electrode Surfaces*, Wiley, New York, 1992, pp. 119–158.
[9] R.A. Mackay, *Colloids Surfaces*, 82 (1994) 1.
[10] J.F. Rusling, in B.E. Conway and J.O'M. Bockris (eds.), *Modern Aspects of Electrochemistry*, No. 26, 1994, pp. 49–104.
[11] M.D. Porter, T.B. Bright, D.L. Allara and C.E.D. Chidsey, *J. Am. Chem. Soc.*, 109 (1987) 3559.
[12] L. Netzer and J. Sagiv, *J. Am. Chem. Soc.*, 105 (1983) 674.
[13] J.F. Rusling and H. Zhang, *Langmuir*, 7 (1991) 1791.
[14] Y. Ohsawa and S. Aoyagui, *J. Electroanal. Chem.*, 145 (1983) 109.
[15] M.J. Eddowes and M. Gratzel, *J. Electroanal. Chem.*, 152 (1983) 143.
[16] M.J. Eddowes and M. Gratzel, *J. Electroanal. Chem.*, 163 (1984) 31.
[17] J.F. Rusling, C.-N. Shi and T.F. Kumosinski, *Anal. Chem.*, 60 (1988) 1260.
[18] A.P. Abbott, G. Guonili, J.M. Bobbitt, J.F. Rusling and T.F. Kumosinski, *J. Phys. Chem.*, 96 (1992) 11091.
[19] J.F. Rusling, H. Zhang and W.S. Willis, *Anal. Chim. Acta*, 235 (1990) 307.
[20] A. Marino and A. Bratjer-Toth, *Anal. Chem.*, 65 (1993) 370.
[21] T.T.-T. Li and M.J. Weaver, *J. Am. Chem. Soc.*, 106 (1984) 6107.
[22] C. Miller, P. Cuendet and M. Gratzel, *J. Phys. Chem.*, 95 (1991) 877.
[23] C.E.D. Chidsey, C.R. Bertozzi, T.M. Putvinski and A.M. Mujsce, *J. Am. Chem. Soc.*, 112 (1990) 4301.
[24] (a) C.E.D. Chidsey, *Science*, 251 (1991) 919; (b) A. Haran, D.H. Waldeck, R. Naaman, E. Moons and D. Cahen, *Science*, 263 (1994) 946.
[25] (a) M. Fujihara and T. Araki, *Chem. Lett.*, (1986) 921; (b) C.A. Widrig, C.J. Miller and M. Majda, *J. Am. Chem. Soc.*, 111 (1988) 2009; (c) X. Zhang and A.J. Bard, *J. Am. Chem. Soc.*, 111 (1989) 8098.
[26] J.F. Rusling, *Microporous Mater.*, (1994) in press.

[27] J.F. Rusling and A.-E.F. Nassar, *J. Am. Chem. Soc., 115* (1993) 11891.

[28] J.F. Rusling, A.-E.F. Nassar and T.F. Kumosinski, in T.F. Kumosinski and M.N. Liebman (eds.), *Molecular Modeling,* Am. Chem. Soc. Symposium Series, 1994, in press.

[29] N. Hu, D.J. Howe, M.F. Ahmadi and J.F. Rusling, *Anal. Chem., 64* (1992) 3180.

[30] A.B.P. Lever, E.R. Milaeva and G. Speier, in C.C. Leznoff and A.B.P. Lever (eds.), *Phthalocyanines,* Vol. 3, VCH, New York, 1993, pp. 1–70.

[31] U. Ahrens and H. Kuhn, *Z. Phys. Chem., Neue Folge, 37* (1963) 1.

[32] M. Seralathan, R.A. Osteryoung and J.G. Osteryoung, *J. Electroanal. Chem., 222* (1987) 69.

[33] J.G. Osteryoung and J.J. O'Dea, in A.J. Bard (ed.), *Electroanalytical Chemistry,* Vol. 14, Marcel Dekker, New York, 1986, pp. 209–308.

[34] J.F. Nagle, *Annu. Rev. Phys. Chem., 31* (1980) 157.

[35] M.J. Stillman and T. Nyokong, in C.C. Leznoff and A.B.P. Lever (eds.), *Phthalocyanines,* Vol. 1, VCH, New York, 1989, pp. 133–289.

[36] R.J. Blagrove and L.C. Gruen, *Aust. J. Chem., 25* (1972) 2553.

[37] R.W. Murray, in A.J. Bard (ed.), *Electroanalytical Chemistry,* Vol. 13, Marcel Dekker, New York, 1984, pp. 191–368.

[38] J.F. Rusling, *CRC Crit. Rev. Anal. Chem., 21* (1989) 49.

[39] A.J. Bard and L.R. Faulkner, *Electrochemical Methods,* Wiley, New York, 1980.

[40] G. Inzelt, in A.J. Bard (ed.), *Electroanalytical Chemistry,* Vol. 18, Marcel Dekker, New York, 1994, pp. 89–241.